Articles

Contribution from the Molecular Spectroscopy Division, National Bureau of Standards, Gaithersburg, Maryland 20899, and Department of Chemistry, Bar Ilan University, Ramat Gan, Israel

Electronic and Geometric Structures of $Pt(NH_3)_2^{2+}$, $Pt(NH_3)_2Cl_2$, $Pt(NH_3)_3X$, and $Pt(NH_3)_2XY$ (X, Y = H_2O, OH^-)

HAROLD BASCH,[†] M. KRAUSS,*[‡] W. J. STEVENS,[‡] and DRORA COHEN[§]

Received October 12, 1984

Isomeric energies and conformations for $Pt(NH_3)_2^{2+}$ (DP), $Pt(NH_3)_2Cl_2$ (DDP), $Pt(NH_3)_3X$, and $Pt(NH_3)_2XY$ (X = NH_3, H_2O, OH^-; Y = H_2O, OH^-) have been calculated by ab initio molecular orbital theory using energy gradient methods. The trends in metal–ligand bond lengths follow a consistent pattern that permits the development of a trans-influence ordering of ligands. The OH^- ligand is predicted to be in an unusual position in this ordering. However, the experimentally derived ordering schemes may not have been examining the bare hydroxy species, which is found to seek out hypervalent hydrogen-bonded attachments. The $Pt(NH_3)_2^{2+}$ fragment is found to have a locally stable "cis" conformation, but the *trans*-DP and all the *trans*-$Pt(NH_3)_2XY$ complexes with X, Y = H_2O, OH^- are lower in energy than the cis. However, with the ionic ligands, Cl and OH, strong hydrogen bonds are obtained for favorable geometric configurations. When these bonds are formed, little difference is found between the energies of the cis and trans isomers.

Introduction

The development of relativistic effective potentials (REP's) to replace the core electrons in high-Z atoms now pemits ab initio calculations of structural and energetic data for heavy-metal complexes. Recently, structural information calculated for square-planar compounds, $Pt(PH_3)_2XY$ (X, Y = H^-, Cl^-), was compared to exptl. data.[1,2] Such molecular orbital calculations permit a direct comparison of the isomeric structural and energy differences for the isolated complexes. Unfortunately, the intepretation of the experimental data is complicated by solvent or crystal interactions, which are absent in the calculated results.

The $Pt(NH_3)_2Cl_2$ (DDP) and $Pt(NH_3)_2XY$ (X, Y = H_2O, OH^-) complexes were chosen for study here because of the interest in these systems as antitumor drugs.[3] The study of the electronic structures, conformations, and relative energetics of these compounds was preliminary to a study of the bonding of the $Pt(NH_3)_3^{2+}$ fragment to ring compounds that model the pyrimidine and purine bases of DNA.

An interesting aspect of the antitumor activity of these drugs is that only the cis compounds are observed to inhibit tumor growth. There is much evidence that this is due to the steric effects of binding to the bases of DNA.[3] Nonetheless, the isomeric energy differences are still of concern and may play a role in relative reactivities. In aqueous solution DDP is hydrolyzed, and although all the hydroxy and aquo species are present,[4,5] the corresponding cis–trans isomers may not be in equilibrium. Since H_2O and OH^- are readily labilized ligands, it is widely assumed that they are the leaving ligands in reaction with the bases. However, the pure aquo–hydroxy species are difficult to isolate because of this lability, and a tendency is found for the hydroxy species to form bridged binuclear and higher order metal complexes at high concentrations. These pure species can be easily studied by the theoretical methods used in this work.

The ab initio calculations reported here explore the cis–trans energetics and the isomeric effect on equilibrium bond distances. In solution, the trans influence of OH^- is usually found to be comparable to that of H_2O and less than that of NH_3.[6] The present calculations show that OH^- has trans influence greater than NH_3 for isolated square-planar platinum(II) complexes. Strong hydrogen bonds are found for appropriate conformations with ionic ligands. This bonding strongly affects cis–trans energetics and the equilibrium bond angles.

Table I. Gaussian Exponents and (Unnormalized) Contraction Coefficients

Pt	5d	19.78	−0.007 224 6
		2.095	0.287 110 2
		0.7435	0.548 015 8
	5d′	0.2257	1.0
	6s	0.9289	1.0
	6s′	0.1326	1.0
	6s″	0.04846	1.0
	6p	1.452	−0.024 304 4
		0.1258	0.368 703 7
	6p′	0.03554	1.0
N	2s	34.91	−0.014 501 2
		6.471	−0.097 926 0
		0.7166	0.550 316 9
	2s′	0.2190	1.0
	2p	16.76	0.028 831 9
		3.602	0.177 510 0
		0.9412	0.496 710 7
	2p′	0.2446	1.0
O	2s	37.91	−0.017 432 1
		8.807	−0.094 327 4
		0.9473	0.575 408 8
	2s′	0.2860	1.0
	2p	20.74	0.033 037 9
		4.633	0.191 044 3
		1.223	0.497 919 2
	2p′	0.3074	1.0

Method of Calculation

The REP for the Pt atom, based on earlier work,[7] has been recently summarized.[8] The (nonrelativistic) chlorine atom potential (for the [Ne]

[†] Bar Ilan University; National Foundation for Cancer Research Associate at NBS.
[‡] NBS.
[§] Bar Ilan University.

(1) Noell, J. O.; Hay, P. J. *Inorg. Chem.* **1982**, *21*, 14.
(2) Kitaura, K.; Ubara, S.; Morokuma, K. *Chem. Phys. Lett.* **1981**, *77*, 452.
(3) See: Lippard, S. J., Ed. "Platinum, Gold, and Other Metal Chemotherapeutic Agents"; American Chemical Society: Washington, DC, 1983; ACS Symp. Ser. No. 209.
(4) Martin, R. B. In ref 3, p 231.
(5) Howe-Grant, M. E.; Lippard, S. J. "Metals in Biological Systems"; Sigel, H., Ed.; Marcel Dekker: New York, 1980; Vol. II, p 63.
(6) Hartley, F. R. "The Chemistry of Platinum and Palladium"; Wiley: New York, 1973; p 301.
(7) Basch, H.; Topiol, S. *J. Chem. Phys.* **1979**, *71*, 802.

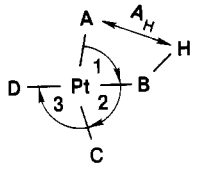

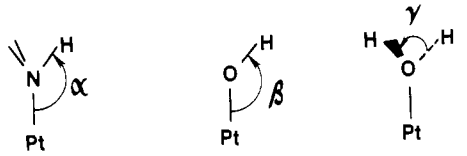

Figure 1. Geometric parameters. $Pt(NH_3)_2^{2+}$, $Pt(NH_3)_2Cl_2$, $Pt(NH_3)_2(H_2O)_2^{2+}$, and $Pt(NH_3)_2(OH)_2$ all have C_{2v} or C_{2h} symmetry. For these conformations the angles and distances depicted are unique with the understanding that all N–H distances in a given NH_3 ligand are equal, as are all OH distances in a given H_2O ligand. A_H is the hydrogen bond distance from A to a H in the plane, or if the bond is a bifurcated type (e.g., to the two H atoms in H_2O), it is the distance in the plane of the line from A, which bisects the line between the two H's. The remaining complexes, $Pt(NH_3)_2(H_2O)OH^+$, $Pt(NH_3)_3OH^+$, and $Pt(NH_3)_3H_2O^{2+}$, all have C_s symmetry. For the $(H_2O)OH$ complexes, two OH bond lengths and angles are obviously needed and the Pt–N–H angles are different for each ammonia ligand. For the triammine complexes there are analogous differences for NH bond lengths and angles. These values will be listed in order of their appearance as we go around the square complex, starting at A, in clockwise fashion. the symmetries of the complexes and the ordering of the ligands are also given in Table III.

core) was taken from Hay et al.,[9] while for nitrogen and oxygen the [He] core potential was taken from the tabulation for Topiol et al.[10] The $(3^s3^p4^d)$ Gaussian primitive exponents for the Pt atom basis set given previously[7] were used in atom calculations for the $5d^96s^1$ (^3D) and $5d^96p^1$ (^3F) states to obtain the contraction coefficients for the final $[3^s2^p2^d]$ basis. For oxygen and nitrogen a (4^s4^p) Gaussian set was exponent optimized for the respective atom ground states and contracted to double-ζ $[2^22^p]$ size. The basis for Pt, O, and N are shown in Table I. For the chlorine atom the basis set was taken directly from Noell and Hay,[1] while for the hydrogen atom Huzinag's[11] (4^s) term was contracted to $[S^s]$ and scaled by the usual $(1.2)^2$ factor.

The ground-state geometries of *trans*-$Pt(NH_3)_2Cl_2$ (C_{2h}), *cis*-$Pt(NH_3)_2Cl_2$ (C_{2v}), *trans*-$Pt(NH_3)_2(H_2O)_2^{2+}$ (C_{2h}), *cis*-$Pt(NH_3)_2(H_2O)_2^{2+}$ (C_{2v}), *trans*-$Pt(NH_3)_2(OH)_2$ (C_{2h}), *cis*-$Pt(NH_3)_2(OH)_2$ (C_{2v}), *trans*-$Pt(NH_3)_2(H_2O)(OH)^+$ (C_s), *cis*-$Pt(NH_3)_2(H_2O)(OH)^+$ (C_s), $Pt(NH_3)_3(H_2O)^{2+}$ (C_s), and $Pt(NH_3)_3(OH)^+$ (C_s) were determined by gradient optimization of all the atom coordinates within the single-configuration Hartree–Fock self-consistent-field (SCF) method using the respective point group symmetries indicated in the parentheses. The constraints implied by the imposed point group symmetries are that (a) the Pt atom and the four ligand atoms directly bonded to it form a plane, (b) the H atom in OH lies in the sample plane, (c) the two hydrogen atoms of H_2O lie symmetrically above and below the plane, and (d) one H atom of NH_3 is in the plane and the other two lie symmetrically abov and below it. These constraints, for example, do not allow the (in-plane) hydrogen atoms in NH_3, H_2O, or OH^- to rotate out of the plane. In addition to the above the optimizations, the linear (trans) and bent (cis) optimized geometries for $Pt(NH_3)_2^{2+}$ and the transition energy curve connecting these configurations were determined. The resultant total energies for all these systems are listed in Table II and corresponding optimized geometric parameters are displayed in Figure 1 and Table III. The conformations for complex Va and Vb are given explicitly in Figure 2 to illustrate Table III. All calculations were carried out by using the GAMESS[12] or HONDO[13] system of programs.

Table II. Energies of Pt Complexes

	E, au		$E_{cis} - E_{trans}$, kcal
	cis	trans	
$Pt(NH_3)_2^{2+}$	−49.5643	−49.5998	22
$Pt(NH_3)_2Cl_2$	−80.8061	−80.8352	18
$Pt(NH_3)_2(OH)_2$	−82.9722[a]	−83.0130	26
	−83.0119[b]		~0
$Pt(NH_3)_2(H_2O)_2^{2+}$	−83.6268	−83.6264	~0
$Pt(NH_3)_2(H_2O)(OH)^+$	−83.3957[c]	−83.4014	4
	−83.3974[d]	83.4014	2
$Pt(NH_3)_3(H_2O)^{2+}$	−78.18949		
$Pt(NH_3)_3(OH)^+$	−77.95841		

[a] Structure IVb, Table III, no H bond. [b] Structure IVa, Table III, H-O--HNH_2 bond. [c] Structure Vb, Table III, H-O--$(H)_2O$ bond. [d] Structure Va, Table III, H-O--HNH_2 bond.

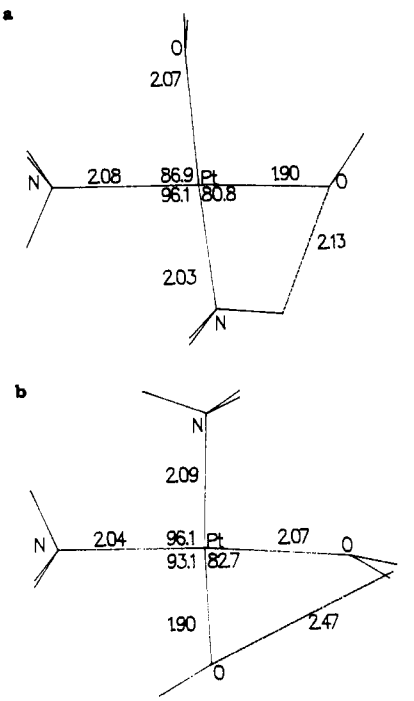

Figure 2. Conformations Va and Vb of Table III, with all distances and angles given except for those required for the bonds to the hydrogen atoms. The hydrogen bonding distance, A_H, is given, though, with the bond shown as a dashed line.

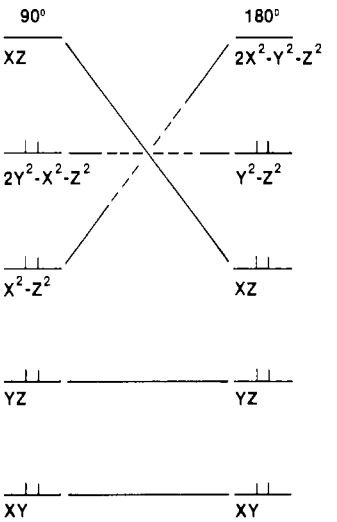

Figure 3. Correlation diagram for the Pt d orbitals describing the orbital transformations that occur for the cis–trans isomerization of $Pt(NH_3)_2^{2+}$. The doubly occupied orbitals in the lowest energy SCF electronic configurations for the cis (90°) and trans (180°) conformations are indicated by the double bars.

(8) Basch, H.; Cohen, D.; Topiol, S. *Isr. J. Chem.* **1980**, *19*, 233.
(9) Hay, P. J.; Wadt, W. R.; Kahn, L. R. *J. Chem. Phys.* **1978**, *68*, 3059.
(10) Topiol, S.; Moscowitz, J. W.; Merlin, C. F. *J. Chem. Phys.* **1979**, *70*, 3008.
(11) Huzinaga, S. *J. Chem. Phys.* **1965**, *42*, 1293.

Table III. Equilibrium Geometries of the Complexes[a]

				A	B	C	D
Ia	C_{2v}	cis	$Pt(NH_3)_2^{2+}$	N	N		
Ib	C_{2i}	trans	$Pt(NH_3)_2^{2+}$	N	N		
IIa	C_{2v}	cis	$Pt(NH_3)_2Cl_2$	Cl	N	N	Cl
IIb	C_{2h}	trans	$Pt(NH_3)_2Cl_2$	Cl	N	Cl	N
IIIa	C_{2v}	cis	$P(NH_3)_2(H_2O)_2^{2+}$	O	N	N	O
IIIb	C_{2h}	trans	$P(NH_3)_2(H_2O)_2^{2+}$	O	N	O	N
IVa	C_{2v}	cis	$Pt(NH_3)_2(OH_2$ (H bond)	O	N	N	O
IVb	C_{2v}	cis	$Pt(NH_3)_2(OH)_2$ (no H bond)				
IVc	C_{2h}	trans	$Pt(NH_3)_2(OH)_2$	O	N	O	N
Va		cis	$Pt(NH_3)_2(H_2O)(OH)^+$	O_2	O_1	N	N
Vb		cis	$Pt(NH_3)_2(H_2O)(OH)^+$	N	O_2	O_1	N
Vc		trans	$Pt(NH_3)_2(H_2O)(OH)^+$	O_1	N	O_2	N
VI			$Pt(NH_3)_3OH^+$	O	N	N	N
VII			$Pt(NH_3)_3H_2O^{2+}$	O	N	N	N

	A	B	C	D	O_H	N_H	A_H	1	2	3	α	β	δ
Ia	2.01	2.01				1.04		94			114.4		
Ib	2.03		2.03			1.04		180			112.3		
IIa	2.29	2.08	2.08	2.29		1.02		83.9	96.4	83.9	116.7		
IIb	2.32	2.04	2.32	2.04		1.02		90	90	90	109.5		
IIIa	2.06	2.03	2.03	2.06	0.99	1.03		88.3	93.3	88.3	114.9		110.5
IIIb	2.05	2.05	2.05	2.05	0.99	1.03	2.67	90	90	90	247.8		111.2
IVa	1.94	2.08	2.08	1.94	0.97	1.01	2.15	81.3	97.8	81.3	260.8	246.9	
						1.03							
IVb	1.92	2.11	2.11	1.92	0.97	1.02		89.0	96.2	89.0	114.0	115.8	
IVc	1.96	2.05	1.96	2.05	0.97	1.02	2.19	82.0	98.0	92.0	258.5	244.6	
Va	2.07	1.90	2.03	2.08	0.98	1.02	2.13	96.2	80.8	96.1	257.9	241.6	111.9
					0.98	1.03					112.3		
Vb	2.09	2.07	1.90	2.04	0.97	1.02	2.47	88.1	82.7	93.1	115.0	121.7	108.6
					0.99	1.02					245.1		
Vc	1.89	2.05	2.10	2.06	0.97	1.02	2.22	82.5	92.8	90.3	256.5	241.9	112.0
					0.98						111.1		
VI	1.90	2.04	2.10	2.08	0.97	1.03		78.7	93.8	94.3	261.2	239.7	
											113.9		
											244.5		
VII	2.07	2.06	2.04	2.06	0.99			89.0	91.7	89.7	114.7		110.6
											246.1		
											111.2		

[a] All distances rounded off to the nearest 0.01 Å. See Figure 1 for header notation.

Conformation and Energetics

a. $Pt(NH_3)_2^{2+}$ (DP). The SCF-optimized trans structure is calculated to be about 22 kcal mol^{-1} more stable than the (local minimum) cis geometry (Table II). This result raises the question of the energetics of isomerization. If the cis–trans interconversion is SCF-calculated as a function of bond angle, θ, with all the other geometric parameters held constant (R_{Pt-N} = 2.052 Å, R_{N-H} = 1.0173 Å, ∠HNH = θ_{tet}), then the orbital correlation diagram shown in Figure 3 (focusing only on the Pt 5d electron molecular orbitals) and the state energy diagram in Figure 4 are obtained. In these figures the molecular X axis coincides with one of the Pt–N bonds, and the other NH_3 bends in the XZ plane. Thus, at θ = 180° (trans) the empty d orbital (for the Pt^{2+} $5d^8$ electronic configuraiton) is the $5d_{2x^2-y^2-z^2}$, while at θ = 90° (cis) the empty d orbital is the $5d_{xz}$. The lowest energy SCF wave functions thus have different d-orbital occupancy, as indicated in the correlation diagram, and the barrier arises because the cis → trans isomerization is a "forbidden" process in the Woodward–Hoffmann sense. The SCF energies are seen to cross in the neighborhood of 130° in Figure 4, with a barrier of ~19 kcal mol^{-1} relative to the cis form. Thus, at the SCF level, a large barrier is found which effectively prevents cis → trans isomerization at room temperature. Five configuration–multiconfiguration SCF (MCSCF) calculations, using all possible distributions of the electron pair "hole" among the five metal d orbitals, allow the orbital population to be determined by minimization of the energy as a function of the bond angle. Between 110 and 120° rapid shifts in population of the $5d_{xz}$ and other orbitals occur which permit an adiabatic transition from 90 to 110° with a barrier of only 7 kcal mol^{-1} (Figure 3). Although inclusion of correlation in a limited MCSCF framework significantly reduces the barrier, 7 kcal mol^{-1} may still be large enough to hold DP in the cis conformation (from a kinetic point of view) if it were initially formed that way.

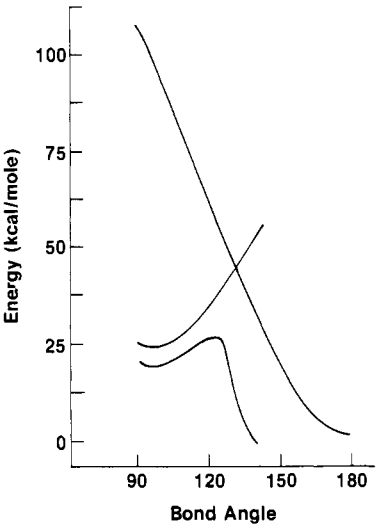

Figure 4. Energy curves for the cis–trans isomerization of $Pt(NH_3)_2^{2+}$. The upper intersecting curves are from SCF calculations with the orbital occupancies determined at either 90 or 180°. The lower curve is obtained with a five-configuration MCSCF calculation which allows for a smooth transformation of the configuration from 90 to 180°.

Although the trans complex is lower in energy than the cis, the Pt–N distance is calculated to be slightly larger for the trans. These Pt–N distances are used as the reference values for gauging

(12) Dupuis, M.; King, H. F. *Int. J. Quantum Chem.* **1977**, *11*, 613; *J. Chem. Phys.* **1978**, *68*, 3998.
(13) Dupuis, M.; Spangler, D.; Wendoloski, J. NRCC Software Catalogue, 1980; Vol. 1, Program No. QG01 (GAMESS).

the *trans* influence of NH_3 and other ligands in the other complexes. Experimental distances are available for comparison with only the crystalline dichlorodiamine complex.[14]

b. *cis*- and *trans*-$Pt(NH_3)_2Cl_2$ (DDP). The larger trans effect of the Cl^- ligand relative to that of ammonia is reflected in the larger Pt–N distance in *cis*-DDP over that in *trans*-DDP. The ratio *cis*/trans Pt–Cl distances is less than unity for DDP, which also reflects the smaller trans influence of NH_3 relative to Cl. An uncritical comparison with experimental metal–ligand bond distances in the crystal for *cis*-DDP would be disappointing, since the ratio of experimental cis/trans Pt–N distances is less than 1. However, the bond lengths for the two Pt–N bonds in the cis complex are reported to be unequal by about 0.1 Å, the Pt–Pt distance between complexes is about 3.4 Å, and intermolecular hydrogen-bonded interactions are likely between the Cl^- anion and NH_3. These interactions between neighboring complexes may be sufficient to make a comparison difficult with the theoretical results for isolated molecules. However, the calculated 2.32-Å Pt–Cl and 2.04-Å Pt–N bond lengths in *trans*-DDP are very close to the observed distances in $PtCl_4^{2-}$ (2.32 Å)[15] and $Pt(NH_3)_4^{2+}$ (2.05 Å),[16] where neighboring interactions are less severe.

For DDP the trans isomer is also calculated to be more stable than the cis isomer by about 19 kcal mol^{-1}. The energetic difference between the isomers appears to be dominated by electrostatic effects, which give a more favorable ligand–ligand interaction in *trans*-DDP, where the anions are further apart. The energy of the cis isomer is stabilized by hydrogen bonds between the Cl ligand and a bifurcated pair of H atoms on the NH_3 ligand, as indicated by the small N–Pt–Cl angle of 83.9°. The comparable cis–trans energy difference between DP and DDP shown in Table II is due, in part, to the stablization of the cis isomer by hydrogen bonding. The hydrogen bond exists even when the N–Pt–Cl angle is 90°, for the total energy of the square-planar conformation is only 2.5 kcal mol^{-1} higher than the value of the optimized conformation. The asymmetry of the cis complex is indicative of the strong intramolecular hydrogen bonds between Cl^- and NH_3 ligands.

c. Aqua and Hydroxy Species: $Pt(NH_3)_2XY$ (X = NH_3, H_2O, OH^-; Y = H_2O, OH^-). The *cis*- and *trans*-diaquo complexes, obtained by the replacement of both Cl ligands in DDP by H_2O, give structures that exhibit the larger trans influence of NH_3 compared to that of H_2O. Thus, the trans Pt–N bond length stays about the same while the cis Pt–N distance decreases in going from the dichloride to $Pt(NH_3)_2(H_2O)_2^{2+}$. Of equal interest is the near equality (in the range 2.03–2.06 Å) of the Pt–NH_3 and Pt–OH_2 bond lengths. This near equality has also been observed in α-pyridonate-bridged *cis*-$Pt(NH_3)_2^{2+}$ complexes[17] (in the range 2.03–2.05 Å). The calculated $Pt(NH_3)_3(H_2O)^{2+}$ complex shows a similar trend (Figure 1) with a 2.04–2.07-Å Pt–N and Pt–O bond length range. In going from the optimized *free* H_2O ligand to the complexed ligand, the water HOH bond angle is calculated to open by 3° (108 → 111°) and the equilibrium OH bond length to increase from 0.98 to 0.99 Å.

The geometry-optimized *trans*-$Pt(NH_3)_2(H_2O)_2^{2+}$ complex is found to have exact 90° O–P–N bond angles, which indicates an absence of significant ligand–ligand interactions. Since this is not found for the corresponding hydroxy complexes, the adjacent $(H_2)O\cdots H(NH_2)$ distance of 2.67 Å in the *cis*-diaquo complex can be used as a reference guide for hydrogen-bond interactions (or their absence) in the hydroxy complexes.

The calculated equilibrium geometry of *trans*-$Pt(NH_3)_2(OH)_2$ in Table III clearly shows the structural effects of intracomplex hydrogen bonds between adjacent NH_3 and OH^- groups. The equilibrium $(H)O\cdots H(NH_2)$ distance for the cis ligands is calculated to be 2.19 Å. Since the point-group symmetry constraints used here do not allow the ammonia groups to rotate about the Pt–N bond axis, it is possible to initially orient the NH_3 groups in a way that such hydrogen bonding with a cis-located OH^- group is physically not possible. Optimized structures for both such arrangements (with and without H bonding) are shown for *cis*-$Pt(NH_3)_2(OH)_2$. The hydrogen-bonded system is characterized by smaller O–Pt–N and Pt–N–H(··O) bond angles while the Pt–O bond length decreases slightly and the Pt–N bond length increases from 2.08 to 2.11 Å. Conformation IVb, with no H bonding, is used to characterize the OH trans influence. As can be seen from Table II, by comparison of the energies for the two *cis*-$Pt(NH_3)_2(OH)_2$ structures, the (two) intramolecular hydrogen bonds are worth ~ 26 kcal mol^{-1}, or ~ 13 kcal mol^{-1} each, which is substantial.

An analogous result is found for the mixed $Pt(NH_3)_2(H_2O)(OH)^+$ complex, where in the trans form the $(H)O\cdots H(NH_2)$ distance is 2.22 Å and the ∠OPtN is 82.5°. In the cis form again two optimized structures were obtained, but here, where the $(H)O\cdots H(NH_2)$ interaction is not available, the system finds an alternative in the $(H)O\cdots H_2(O)$ "double" hydrogen bond. In consequence, the angle between the $Pt–O(H_2)$ bond and the OH_2 plane is only 131.2° as compared to a normal 180° in the other aquo complexes. As can be seen from the energetics in Table II, apparently the $(H)O\cdots H(NH_2)$ and "doublet" $(H)O\cdots H_2(O)$ interaction energies are comparable and the two *cis*-$Pt(NH_3)_2(H_2O)(OH)^+$ structures are of about the same energy.

The $Pt(NH_3)_3(OH)^+$ complex shows the strongest intraligand hydrogen bond interaction, as judged by the internal angles of the cyclic hydrogen bond network. Thus ∠OPtN is now 78.7° and ∠PtNH is 98.8°, reduced from 105.0° in *trans*-$Pt(NH_3)_2(OH)_2$ and the usual 110–116° in the other coordinated ammonias. The Pt–N distance remains within the usual 2.04–2.06-Å range found for NH_3 trans to NH_3.

Ammonia trans to OH^-, however, is calculated to have longer Pt–N bond distances, in the 2.09–2.11-Å range, which are larger than for any other *trans* ligand studied here. This establishes OH^- as the strongest *trans*-influencing ligand in the order $OH^- > Cl^- > NH_3 > H_2O$. This calculated ordering agrees with the conventional one[6] except for OH^-, which is usually considered to be about the same as H_2O. The discrepancy is probably connected with the difficulty in experimentally characterizing hydroxy complexes.[4,18] There are also apparently no reported crystal structures for mononuclear aquo or hydroxy complexes. In a hydroxy-bridged binuclear complex a Pt–O distance of 2.03 Å is reported.[18] A Pt–O bond length of ~2.00 Å in the other oxygen-containing anionic ligand–Pt complexes has also been reported.[19] As can be seen in Table III, the Pt–O distance in the hydroxy complexes studied here fall in the 1.89–1.97-Å range, with the higher value calculated for OH^- as the trans ligand to OH^-.

The strong intraligand hydrogen bonding found here for the mononuclear square-planar Pt(II) complexes involving only the hydroxy ligand shows that OH^- is too "reactive" to exist as an isolated, noninteracting ligand. This possibly explains the tendency toward hydroxy-bridged binuclear and higher-nuclear metal complexes found in the crystal structures and in aqueous solutions. It also suggests that the "naked" OH^- ligand does not exist, as such, in solution and must be strongly bound to the solvent or to other ligands. This would explain its weaker trans-influencing strength derived experimentally relative to that found here.

The isomeric energy differences in Table II for these molecules support the contention that ligand–ligand (electrostatic) interactions dominate these energies. The DP and DDP complexes exhibit large and comparable isomeric energy differences on the SCF level. Substitution of H_2O for Cl^- strongly reduces the cis–trans energy difference by diminishing the electrostatic advantage of the trans species. The hydroxy and mixed hydroxy–aquo complex isomer energy differences are small. In the di-

(14) Millburn G. H.; Truter, M. R. *J. Chem. Soc.* **1966**, 1609.
(15) Atoji, M.; Richardson, J. W.; Rundle, R. E. *J. Am. Chem. Soc.* **1957**, *79*, 3017.
(16) Shandles, R.; Schlemper, E. O.; Murmann, R. K. *Inorg. Chem.* **1971**, *10*, 2785.
(17) Hollis, L. S.; Lippard, S. J. *J. Am. Chem. Soc.* **1983**, *105*, 3494.
(18) Faggiani, R.; Lippert, B.; Locke, C. J. L.; Rosenberg, B. *J. Am. Chem. Soc.* **1977**, *99*, 777.
(19) Carrondo, M. A. A. F. d. C. T.; Goodgame, D. J. L.; Hadjioannon, C. R.; Skapski, A. C. *Inorg. Chim. Acta* **1980**, *46*, L32.

hydroxy case this is presumably due to the same strong, dominating intraligand hydrogen-bond network in both isomers, which also keeps the adjacent OH^- ligands farther from each other.

Acknowledgment. H.B. is a Research Associate at the NBS supported by a contract with the National Foundation for Cancer Research.

Registry No. IIa, 15663-27-1; IIb, 14913-33-8; IIIa, 20115-64-4; IIIb, 20115-65-5; IVb, 63700-88-9; IVc, 97805-43-1; Va, 54933-51-6; Vc, 54906-64-8; VI, 97732-33-7; VII, 17524-19-5.

Contribution from the Division of Chemistry,
National Research Council of Canada, Ottawa, Ontario, Canada K1A 0R9

EPR Spectra and Structures of Three Binuclear Nickel Carbonyls Trapped in a Krypton Matrix: $Ni_2(CO)_8^+$, $Ni_2(CO)_7^-$, and $Ni_2(CO)_6^+$ †

J. R. MORTON* and K. F. PRESTON

Received November 2, 1984

Three binuclear nickel carbonyl free radicals have been detected by EPR spectroscopy in a Kr matrix at 77 K. The observed spectra are tentatively assigned to the species $Ni_2(CO)_8^+$, $Ni_2(CO)_7^-$, and $Ni_2(CO)_6^+$, which have two, one, and two bridging carbonyls, respectively.

Introduction

In our studies of paramagnetic metal carbonyls, we recently turned our attention to the EPR spectra of cluster species. This topic was initiated with our investigation[1] of the binuclear manganese carbonyl $Mn_2(CO)_9^-$ in a single crystal of $Mn_2(CO)_{10}$. With the discovery[2] of $HCo_2(CO)_8$ and $Co_2(CO)_8^-$ as products of the γ irradiation of $HCo(CO)_4$ in Kr, it became apparent that clustering of metal carbonyls occurred in a krypton matrix at 77 K. The γ irradiation of metal carbonyls in Kr thus offered a potentially fruitful source of polynuclear carbonyl radicals for spectroscopic studies.

In the present article we discuss the structures of three binuclear nickel carbonyl radicals derived from $Ni(CO)_4$.

Experimental Section

Nickel tetracarbonyl was obtained from Alfa Inorganics; nickel metal enriched to 86% in the isotope ^{61}Ni was obtained from Oak Ridge National Laboratory and carbon monoxide enriched to 99% in ^{13}C from Merck Sharp and Dohme Ltd., Montreal, Canada.

$Ni(CO)_4$ enriched in ^{13}C was prepared by thermal decomposition of ordinary $Ni(CO)_4$ in a thick-walled glass tube. After the CO formed was removed, a small quantity of mercury was introduced, followed by excess ^{13}CO. When the tube was heated to 80 °C, at which temperature the pressure was approximately 1 MPa, $Ni(CO)_4$ enriched in ^{13}C was obtained. Enrichment with ^{61}Ni was carried out by reacting enriched metal with CO at 300 °C and 30 MPa with use of a droplet of mercury as a catalyst.

Two micromoles of $Ni(CO)_4$ and 2500 μmol of krypton (Matheson) were placed in a 4 mm o.d. Suprasil tube, which was sealed off under vacuum. The samples were annealed at −130 °C and then irradiated at 77 K in a 700-TBq ^{60}Co γ source.

EPR spectra were obtained at 77 K with a Varian E12 spectrometer equipped with accessories to measure the microwave frequency and the magnetic field. Spectral simulations were carried out with the aid of the Lefebvre–Maruani[5] or Belford[6] programs.

Results

Freshly irradiated samples of $Ni(CO)_4$ in krypton showed, at 77 K, spectra attributable to three species. A very strong signal at $g = 2.1425$ was labeled A but unfortunately could not be positively associated with any other features in the spectrum. Two weaker features at 1.9781 and 2.0000 were associated with species B, and a third species (C) had principal values 2.0186, 2.0055, and 1.9909. After a few hours at 77 K, B had disappeared completely, A had diminished considerably, and C had increased in intensity. When these experiments were repeated with $Ni(CO)_4$ enriched in the isotope ^{61}Ni ($I = {}^3/_2$), all six transitions revealed hyperfine structure characteristic of two equivalent ^{61}Ni nuclei (e.g. Figure 1). It would appear, therefore, that three distinct binuclear species have been generated.

Table I. Spectral Parameters of Species A, B, and C in Krypton at 77 K

species	parameter	*x*	*y*	*z*
A	*g*		2.1425	
	Ni(2)[a]		−15.4	
	C(2)		31.6	
	C(2 or 4)		9.9	
	C(4 or 2)		11.5	
B	*g*	2.0000	2.0000	1.9781
	Ni(2)[a]	−43.9	−43.9	−42.6
	C(1)	?	?	17.8
	C(6?)	?	?	~3
C	*g*	2.0186	2.0055	1.9909
	Ni(2)[a]	∓6.4	∓5.0	±20.3
	C(2)	10.2	8	9.2
	C(4)	5.1	5	1.0

[a] Two ^{61}Ni nuclei have the given hyperfine interaction (gauss). Sign choices for the ^{61}Ni hyperfine components reflect the fact that the magnetic moment of ^{61}Ni is negative.

The results of ^{13}C enrichment experiments will be presented for each species in turn:

In low enrichment (10–15%) the transition at 2.1425 belonging to A was accompanied by three pairs of satellites, indicative of ^{13}C hyperfine interactions of 31.6, 11.5, and 9.9 G. With very high (99%) ^{13}C enrichment the line at 2.1425 was replaced by a wide (over 100 G) manifold of lines approximately 10.5 G apart. A satisfactory simulation of this spectrum was achieved on the assumptions that (a) 2.1425 is a principal *g* value of an orthorhombic tensor, and not the "perpendicular" value of an axial tensor, (b) two ^{13}C nuclei have 31.6-G hyperfine interactions, and (c) two ^{13}C nuclei have 11.5-G hyperfine interactions, and four have 9.9-G interactions, or vice versa.

The spectrum of species B when enriched in ^{13}C revealed the presence of a unique carbon atom whose hyperfine interaction was 17.8 G at $g = 1.9781$. There was also an indication of small (ca. 3 G) hyperfine interactions with several other carbon nuclei, although the precise number of these could not be determined.

† NRCC No. 24884.

(1) Lionel, T.; Morton, J. R.; Preston, K. F. *Inorg. Chem.* **1983**, *22*, 145.
(2) Fairhurst, S. A.; Morton, J. R.; Preston, K. F. *Organometallics* **1983**, *2*, 1869.
(3) Krusic, P. J.; San Filippo, J.; Hutchinson, B.; Hance, R. L.; Daniels, L. M. *J. Am. Chem. Soc.* **1981**, *103*, 2129.
(4) Krusic, P. J. *J. Am. Chem. Soc.* **1981**, *103*, 2131.
(5) Lefebvre, R.; Maruani, J. *J. Chem. Phys.* **1965**, *42*, 1480.
(6) Belford, R. L.; Nilges, M. J. "Computer Simulation of Powder Spectra", EPR Symposium, 21st Rocky Mountain Conference, Denver, CO, Aug 1979.

0020-1669/85/1324-3317$01.50/0